CLM-P 388

A SPECTROSCOPIC STUDY OF THE RECOMBINATION OF C^{6+} TO C^{5+} IN AN EXPANDING LASER-PRODUCED PLASMA

F. E. Irons* and N. J. Peacock

(Submitted for publication in J. Phys. B, Atom. Molec. Phys.)

ABSTRACT

The Lyman spectrum of carbon VI from the expansion plume of a laser-produced plasma has been interpreted to give the absolute distribution of electrons amongst bound and free energy states. Local thermal equilibrium is shown to be attained for bound states equal to and above a certain principal quantum number n which varies with the plasma parameters from $n \simeq 4$ at a distance of 1.0 mm from the target to $n \simeq 6$ at 2.8 mm. At 2.8 mm, excited states of principal quantum number 2 - 5 have an inverted population. Plasma densities ($N_e \simeq 4 - 0.2 \times 10^{18}$ cm^{-3}) and temperatures ($T_e \simeq 38 - 9$ eV) have been deduced from spectral intensities at distances of 1.0 - 2.8 mm from the target. Spectral intensities have also been interpreted in conjunction with plasma parameters and certain theoretical de-excitation rate coefficients to give the (collisional-radiative) recombination coefficient for the recombination of C^{6+} to the hydrogen-like C^{5+}, and this is compared with theory. The coefficient for purely two-body recombination to the ground state of C^{5+} has been deduced from the free-bound continuum intensity and is in good agreement with theory. With increasing distance from the target two-body recombination is seen to become progressively less important compared to three-body recombination, as is predicted by theory for an adiabatic expansion. Over the region 1.0 - 2.8 mm from the target, volume expansion and not recombination is shown to be the major cause of density decay, which is approximately adiabatic.

*Now at the Department of Engineering Physics, Research School of Physical Sciences, Australian National University, Canberra, A.C.T. 2600, Australia.

UKAEA Research Group,
Culham Laboratory,
Abingdon, Berks.

March 1974.

1. Introduction

When a high power laser pulse is focussed onto a solid target in vacuum a plasma is formed which expands away from the target surface, exhibiting a rapid decrease in density which may be attributed to both volume expansion and recombination. For a highly ionised plasma from a multi-Z target, theory indicates that initially there will be a period of rapid recombination, covering the first few millimetres of expansion, after which the degree of ionisation may be "frozen" into the plasma and further recombination will then only take place over a substantially greater distance (Zel'dovich and Raizer, 1967; Burgess et al, 1967; Peacock and Pease, 1969; Mattioli, 1971). Semi-quantitative support for this theory may be adduced from spectroscopic observations which show that the most highly ionised species exist only close to the target (see Peacock and Pease, 1969); from observations of charge collection which show only a limited reduction in ion numbers out to tens of centimetres from the target (Mattioli and Véron, 1971) and from observations of recombination radiation (Boland et al, 1968, Basov et al, 1969). In other circumstances a terminal stage of ionisation may not be reached (Mattioli and Véron, 1969; Sèka et al, 1969).

There is a general lack of data on the electronic recombination of highly-stripped ions in the regime of moderately high density but low temperature (characteristic of the expansion phase of a laser-produced plasma) where three-body recombination makes a major contribution to the nett recombination. This, plus the need to know the rate of recombination in a laser-produced plasma anyway (for example for the utilisation of the plasma as an ion source - see eg. Tonon 1972) has prompted us to examine how a measurement of this rate might be made. We consider specifically the electronic recombination of the ion C^{6+} to the hydrogen-like ion C^{5+} in the plasma produced by the laser irradiation of polyethylene.

Conventionally one would deduce the rate of recombination from an observation of the rate of density decay, allowance being made for the effects of volume

expansion by the use of an appropriate plasma model (eg. Baravian et al, 1973). However because of the limited accuracy inherent in any such model this procedure becomes impractical when recombination is only a minor cause of density decay. It is also impractical when the competing effects of recombination to and from an ion need to be separated (which, as it so happens, is not the case here since we are specifically considering the most highly ionised species). The method to be described (similar to that of Robben et al, 1963; Hinnov, 1966; and Stevefelt and Robben, 1972) is based on a calculation of the various atomic processes which contribute to the recombination, and is possibly the most suitable under the present conditions.

In the density-temperature regime of interest here, according to the collisional-radiative theory of plasma decay (Bates et al, 1962 a, b) electrons are captured principally by the three-body process onto high quantum states of an ion and they then diffuse, mostly with unit change of principal quantum number, down through the excited states by a series of collision induced transitions, with radiative de-excitation becoming increasingly important at lower quantum states. It follows from this theory that the rate of decay can be calculated by choosing any excited state, of principal quantum number n' say, and calculating the amount by which de-excitation from bound states $n \geq n'$ to bound states $n < n'$ exceeds the inverse excitation, and adding on the amount by which direct recombination from free states to bound states $n < n'$ exceeds the inverse ionisation, viz

$$
\begin{aligned}
-\dot{N}(C^{6+}) = & \sum_{n=n'}^{\infty} N_n \left(\sum_{m=1}^{n'-1} \left\{ A(n,m) + K(n,m) N_e \right\} \right) \\
& + N_e N(C^{6+}) \sum_{m=1}^{n'-1} \left\{ K(c,m) + \beta(m) \right\} \\
& - N_e \sum_{m=1}^{n'-1} N_m \left(\sum_{n=n'}^{\infty} K(m,n) + K(m,c) \right) \qquad (1)
\end{aligned}
$$

where $N(C^{6+})$ denotes the number density of the ion C^{6+}

" N_e " the free electron density

" N_n " the population density of the bound state n of C^{5+}

" $A(n,m)$ " the radiative transition probability from state $n \rightarrow m$

" $\beta(m)$ " the two body recombination coefficient to the state m

" $K(n,m)$ " the rate coefficient for the collision induced transition from state $n \rightarrow m$

" $K(c,m)$ and $K(m,c)$ denote the rate coefficients for three-body recombination and collisional ionisation respectively between the continuum and the state m.

The notation for the rate coefficients is the same as that of Bates et al (1962 a, b) except that to be consistent with our earlier publications we use the symbols n, m for principal quantum number rather than p, q.

A theoretical evaluation of $\dot{N}(C^{6+})$ from eqn 1 would proceed by first calculating the excited state densities N_n. This would be accomplished (e.g. Bates et al., 1962a) by a simultaneous solution of the rate equations (one for each bound state) which describe the population and depopulation of each state. Rather severe problems arise however when the reabsorption of spectral line radiation must be included, and only in the more straightforward cases is it possible to proceed (Bates et al, 1962b; Hearn, 1966; Drawin, 1969; Mewe, 1970). This difficulty can however be circumvented by actually measuring N_n, from spectral line intensities. Allowance may have to be made for self-absorption when interpreting line intensities to give N_n but this is a simpler problem than that referred to above: in the present case only the first few excited states are so affected and these will be seen to have a minimal influence on the rate of recombination anyway.

The method to be employed for evaluating $\dot{N}(C^{6+})$ then consists of multiplying the experimental values of population densities by theoretical values of the rate coefficients which appear in eqn 1. The actual rate coefficients used here are the same as those used by Bates et al, 1962a, for hydrogen-like ions. Note that this method can be extended to other ions, except that the rate coefficients for non hydrogen-like ions are not as well known as for hydrogen-like ions.

Although in principle any excited state can be chosen as the state n' for the evaluation of eqn 1, certain states are to be preferred (see e. g. the discussion of Byron et al, 1962, and Griem, 1964, for a fully theoretical evaluation of eqn 1). For the combination experimental-theoretical method described above, n' should not be so great (i. e. not greater than the thermal limit) that eqn 1 involves the difference between two large and nearly equal quantities, each with a significant error; nor should it be so small that the radiative terms which appear in eqn 1 are affected by self-absorption (such effects are not allowed for in eqn 1). These requirements can be met fairly well in the present plasma, with $n' = 3$ and 4.

After a brief description of the experimental arrangement (section 2), results for the distances 1.0, 1.6 and 2.8 mm from the target will be presented (section 3) and analysed (section 4) to give the distribution of electrons amongst bound and free energy states. Plasma parameters, the rate of recombination and the associated recombination coefficients will be deduced, and a comparison will be made with theory.

2. Experimental Arrangement

For full details of the experimental arrangement, including a diagram, reference should be made to an earlier paper (Irons and Peacock, 1973, hereafter called paper A), which describes an application of the present laser-produced plasma as a light source for the branching ratio method of intensity calibration at soft X ray wavelengths. Briefly, the experimental arrangement is as follows.

The plasma is formed by irradiating a polyethylene $(C_2H_4)_n$ target with a pulsed neodymium glass laser beam which is focussed in vacuo ($< 10^{-4}$ torr) through a 10 cm focal length lens at near normal incidence onto the target surface. The laser was switched in the "pulse transmission mode" to give 6J of energy in a pulse of duration 6 ns, rising to peak intensity in 1.5 ns. The focussed laser flux was $\approx 2{\cdot}5 \times 10^{11}$ W cm^{-2}. The laser was brought to a focus on the target at a distance of 4 mm from the entrance slit of a grazing incidence spectrograph. The plasma expands away from the target about an axis which is inclined at a few degrees to the target normal. This axis will be referred to as the x axis (the same as the 'plasma axis' in paper A), and distances along the x axis will be measured with respect to the laser focal point on the target as origin. The x axis is parallel (within a few degrees) to the entrance slit of the grazing incidence spectrograph and is at the centre of the angle of acceptance of the spectrograph. With this arrangement the spectrograph sees light emitted at right angles to the x axis; and a pin hole aperture inserted within the spectrograph gives spatial resolution (0.5 mm) along the x axis.

The grazing incidence spectrograph, of the type described by Gabriel et al (1965), but with the modified entrance slit assembly as described in paper A, was operated at an 88° angle of incidence using a Bausch and Lomb 2 metre radius 600 g/mm gold coated grating. Spectra were recorded on Ilford Q2 emulsion,

for which the non-linear response at densities above 0.2 and up to the maximum recorded here (0.5) was measured by the method described in paper A, and subsequently corrected for. The spectrograph has been used to record the Lyman spectrum of CVI, in the wavelength range 20-34 Å. For a relative intensity calibration over this rather short wavelength range it was considered adequate to use the calibration of Morgan et al (1968) which is for a similar instrument, but refers to a platinum coated grating. Recent measurements (Hobby and Peacock, 1973; and paper A) at seven wavelengths in the range 8-45 Å indicate that the wavelength dependence is substantially the same for a platinum coated grating as for a gold coated grating (as used here), and this result is substantiated by the work of Speer and Turner (1973).

An Ebert monochromator of 1.5 metre focal length has been used to record the lines CV ($2s^3S_1 - 2p^3P_2$) 2271, (6-7) 4945 Å and CVI (6-7) 3434, (7-8) 5290 Å. Light emitted from the plasma at right angles to the x axis was focussed by a quartz-lithium fluoride achromat onto the entrance slit of the monochromator, the signal at the exit slit being monitored by a photomultiplier (EMI 9594 QB) and displayed on a Tektronix 519 oscilloscope. The complete optical system was calibrated for absolute intensity by means of a tungsten strip lamp.

3. Results

We are concerned specifically with the region of plasma emitting CVI radiation. Previous observations on a similar plasma (Irons et al, 1972) have shown that this region is concentrated about the x axis in the shape of a cone, with the apex towards the target, and that the volume of this cone becomes larger with time as it expands away from the target.

The Ebert monochromator was set up to observe the plasma at different distances from the target. In the present experiment luminosity time-of-flight observations, of the line CVI (6-7) 3434 Å, have shown that the CVI emission appears (at each point of observation) as a pulse of duration ~ 11 ns (full width at half peak intensity) and comes from a region of plasma which is streaming away from the target with a mean velocity of $\sim 2.5 \times 10^7$ cm s^{-1}. Surface intensity measurements of CVI (6-7) 3434 and (7-8) 5290 Å have been made and have been averaged in time to give values which, for a line of sight intersecting the x axis, we denote by I_{67} and I_{78} respectively. Spatial scans give the depth of plasma at right angles to the x axis. It might be noted that the above lines are a prominent feature in the visible and near u.v. spectrum of a laser-produced carbon plasma, and that they are strongly Stark broadened (Irons, 1973).

A portion of the spectrum, covering the wavelength range 20-40 Å which includes the Lyman spectrum of CVI, is shown in fig. 1, as recorded with the grazing incidence spectrograph, with spatial resolution over the region 0-5 mm from the target. An entrance slit width of 10 μm, in conjunction with a 34 shot exposure gives good spectral resolution and intensity on the plate, sufficient to detect up to seven series members. The latter is clearly seen in the spectrophotometer scan in fig. 1, which corresponds to a distance of 1.0 mm from the target. The spectral intensities can be seen to decrease rapidly with distance from the target. Some of the lines can be detected beyond the distance of 5 mm indicated in the figure, while the much weaker free-bound continuum cannot be detected at distances much beyond 1.0 mm.

4. Analysis and Discussion

We first consider the interpretation of line and continuum intensities to give the distribution of electrons amongst bound and free energy states (section 4.1). This distribution is then analysed, firstly from the point of view of departure from local thermal equilibrium (section 4.2), and secondly, in conjunction with the electron temperatures and the electron and ion densities deduced from spectral intensities (section 4.3), to give the rate of recombination and the recombination coefficient (section 4.4).

4.1 Interpretation of Intensities

4.1.1 Line Intensities

The surface intensity I_{mn} (ergs s^{-1} cm^{-2} sr^{-1}) of the spectral line of frequency ν_o which results from the transition between bound states of principal quantum numbers n and m is related to the population density N_n of the upper state n by the equation

$$I_{mn} = \frac{A(n,m)\, h\nu_o\, N_n}{4\pi} \times (\text{plasma depth}) \quad . \qquad (2)$$

Photographic densities for the transitions CVI (1-n), n = 2-8, suitably corrected for non-linear emulsion response and the relative intensity response of the grazing incidence spectrograph, provide quantities which, when corrected for self-absorption in the plasma (see below), are proportional to I_{mn}. A division by $\frac{A(n,m)\, h\nu_o}{4\pi}$ then gives quantities which are proportional to N_n, and a further division by the respective statistical weights $\omega_n = 2n^2$ gives the relative values of $\frac{N_n}{\omega_n}$ which are shown in fig. 2, plotted on a log-linear scale as a function of the respective ionisation potentials χ_n. These values have been put on an absolute scale by means of values of $\frac{N_7}{\omega_7}$ and $\frac{N_8}{\omega_8}$ deduced from eqn 2 using values of I_{67}, I_{78} and 'plasma depth' measured

as described in section 3. It might be noted that these measurements are the basis of the branching ratio intensity calibration described in paper A and that, in paper A, good agreement was reported with a second independent method of intensity calibration.

Results are presented in fig. 2 for the three distances x = 1.0, 1.6 and 2.8 mm from the target. At x = 2.8 mm only transitions up to CVI (1-6) could be detected (and even then CVI (1-6) had to be measured relative to (1-5) on a second photographic record, with a 103 shot exposure and a 25μ entrance slit). The photographic densities of these transitions relative to the densities of the corresponding lines at x = 1.0 and 1.6 mm was the basis for the determination of absolute values of $\frac{N_n}{\omega_n}$, n = 2-6, at x = 2.8 mm. The values of $\frac{N_7}{\omega_7}$ and $\frac{N_8}{\omega_8}$ shown in fig. 2 for x = 2.8 mm were deduced from I_{67} and I_{78} respectively.

The correction for self-absorption referred to above stems from a calculation, based on a reasonable plasma model, which is of wider interest than just the present application and will be described elsewhere (Irons, 1975). This calculation incorporates into the equation of radiative transfer the Doppler structure in the line profile due to the plasma streaming motion, and shows how, with a knowledge of the plasma parameters, the intensity of light emitted normal to the x axis can be interpreted to give the average upper state density along the line of sight. There is evidence from a similar plasma (Irons et al, 1972) that the Doppler structure due to the streaming motion is the dominant cause of broadening, in which case the different frequencies which make up the line profile are emitted (and absorbed) in different regions of plasma, and the nett absorption as contained in the total line intensities is a representative spatial average (i.e. the origin of light reaching the observer is not necessarily weighted to the region of plasma closest to the observer). In the present case the correction for self absorption (see Irons, 1975)

consists essentially of multiplying the observed intensities by x 12 (L_α), x 4 (L_β), x 1.6 (L_γ) and x 1.1 (L_δ) at x = 1.0 mm; by x 6 (L_α), x1.7 (L_β) and x 1.2 (L_γ) at x = 1.6 mm; and by x 2 (L_α) and x 1.2 (L_β) at x = 2.8 mm. No correction has been applied to other lines of interest in this paper since theory (Irons, 1975) indicates that these lines have their intensities reduced less than 10% by self-absorption: indeed experimental evidence to this effect, for lines from higher bound states, has been discussed in paper A.

4.1.2 The Free-bound Continuum Intensity

The surface intensity $\varepsilon(\nu)$ (ergs s^{-1} cm^{-2} sr^{-1} per unit frequency interval) of the CVI Lyman free-bound continuum at the frequency ν is related to the number density $dN_e(E)$ of free electrons in the range of kinetic energy E - (E + dE) (where $E = h(\nu - \nu_1)$, with ν_1 equal to the frequency of the continuum edge) by the equation

$$\varepsilon(\nu) = \frac{h\nu}{4\pi} N(C^{6+})\, dN_e(E)\, h\left(\frac{2E}{m}\right)^{\frac{1}{2}} \sigma_{v1} \times (\text{plasma depth}) \qquad (3)$$

where σ_{v1} is the cross section for photorecombination to the ground state (the notation is that of Cooper, 1966, where the subscript v denotes velocity i.e. $\frac{1}{2}mv^2 = E$ and the subscript 1 denotes the ground state). Cooper (1966) gives an expression for σ_{v1} (which we use) obtained by detailed balancing from the photoionisation cross section of Menzel and Pekeris (1935). The gaunt factor which appears in this expression is here put equal to 0.8 (Griem, 1964).

Photographic densities (< 0.2 in magnitude) at a finite number of points in the continuum, suitably corrected for the relative intensity response of the grazing incidence spectrograph, provide quantities which are proportional to $\varepsilon(\nu)$.

A division by $\frac{h\nu}{4\pi}\ h\left(\frac{2E}{m}\right)^{\frac{1}{2}}\sigma_{v1}$ then gives quantities which are proportional to $N(C^{6+})\,dN_e(E)$. A further division by the product $N(C^{6+})\,d\omega_e(E) = 2\omega_i\left(\frac{E}{\pi}\right)^{\frac{1}{2}}\left(\frac{2\pi m}{h}\right)^{\frac{3}{2}}$ (see eg. Griem, 1964) where $d\omega_e(E)$ denotes the appropriate statistical weight of free electrons and ω_i (= 1) denotes the statistical weight of the fully stripped ion, then gives the relative values of $\frac{dN_e(E)}{d\omega_e(E)}$ which are shown in fig. 2, plotted on a log-linear scale as a function of the energy E. These values have been deduced in a consistent manner with those of $\frac{N_n}{\omega_n}$ and the absolute scale on the ordinate in fig. 2 applies to both the bound and free electron distributions. No correction is necessary here for self-absorption since theory indicates that the continuum at x = 1.0 mm is optically thin (paper A). The continuum could not be detected at x = 1.6 mm.

In fig. 2 the continuum edge (≡ series limit) is chosen as the origin of zero energy and the bound state energies are plotted as positive and the free electron energies as negative. Error bars attached to the data points arise mainly from the reduction of the photographic data, including the use of the relative intensity calibration of Morgan et al (1968), for which the error is set equal to zero at the continuum edge and increases to higher and lower wavelengths. Where a correction has been made for self-absorption the amount added to the observed line intensity may be in error by a factor of two, and with some lines, notably L_α, this is the dominant error. In addition to these relative errors there is an error of $\pm$ 30% in the absolute value of each data point (arising from the method of assigning absolute values) which is not shown in the figure.

4.2 Local Thermal Equilibrium

The continuum-derived values of $\frac{dN_e(E)}{d\omega_e(E)}$ at x = 1.0 mm (fig. 2) fall on a straight line, indicating a Maxwellian distribution of free electron energies with a temperature as given by the (inverse) slope of 38^{+}_{-} 4 eV. Thermal equilibrium theory indicates that this line is related to the free electron density and temperature by Maxwell's equation, which may be written as (e.g. Griem, 1964)

$$\frac{dN_e(E)}{d\omega_e(E)} = \frac{N_e}{2} \frac{N(C^{6+})}{\omega_i} \left(\frac{h^2}{2\pi mkT_e} \right)^{\frac{3}{2}} \exp\left(-\frac{E}{kT_e} \right) \quad . \tag{4}$$

A similar theory indicates that in local thermal equilibrium (L. T. E.) the number densities of bound electrons are related to the free electron density and temperature by the Saha-Boltzmann equation (e.g. McWhirter, 1965) viz

$$\frac{N_n}{\omega_n} = \frac{N_e}{2} \frac{N(C^{6+})}{\omega_i} \left(\frac{h^2}{2\pi mkT_e} \right)^{\frac{3}{2}} \exp\left(\frac{\chi_n}{kT_e} \right) \quad . \tag{5}$$

Equations 4 and 5 are similar in form, as is to be expected since they both describe the equilibrium distribution of electrons amongst energy states.

At x = 1.0 mm (fig. 2) a straight line representing eqn 5 has been fitted to the higher bound states, with a slope (ie. temperature) equal to that of the line fitted to the continuum. Where these two lines overlap, at the point $E = \chi_\infty = 0$, they are equal in magnitude (within the experimental error limits). We regard this as confirmation of the formula (Menzel and Pekeris, 1935) for σ_{v1}, and also of the fact that the higher bound states are in L. T. E. and that the line fitted to the higher bound states does indeed represent eqn 5. At x = 1.6 mm and

2.8 mm (fig. 2) straight lines representing eqn 5 have been fitted to the higher bound states and the slope of these correspond to temperatures of 17^{+8}_{-5} eV and 9^{+5}_{-2} eV respectively.

It is of course quite reasonable that the higher bound states should be in L.T.E. with the free electrons since these states, besides being coupled to one another by collisional excitation and de-excitation are coupled to the free electrons by collisional ionisation and three-body recombination. Furthermore, theory (McWhirter and Hearn, 1963) indicates that there is sufficient time for the excited state densities to relax to quasi-steady state values.

For lower quantum states radiative de-excitation becomes increasingly important and it is well known from the collisional-radiative theory of recombination that a state n is reached (the thermal limit) below which significant departure (> 10%) from L.T.E. occurs. According to McWhirter (1965) the state n may be determined from the condition that $\chi(n, n-1)$ should be the greatest excitation potential between neighbouring states which satisfies the inequality

$$N_e \geq 1.73 \times 10^{14} T_e^{\frac{1}{2}} \chi(n, n-1)^3 \qquad (6)$$

where T_e and $\chi(n, n-1)$ are in eV. With the values of N_e and T_e from Table 1 we find n = 5 at x = 1.0 and 1.6 mm, and n = 6 at x = 2.8 mm. At x = 1.0 mm (fig. 2) the lowest quantum state to be within 10% of the L.T.E. value is n = 3 or 4 rather than 5, but this can be attributed to the elevation of the excited state densities N_n, n = 2-5, by the partial absorption of the lower Lyman lines (section 4.1.1); a fact which is not considered in the derivation of the formula in eqn 6. The predicted departure from L.T.E. at x = 1.6 and 2.8 mm was taken into account when selecting the straight lines of best fit to the higher bound states in fig. 2.

The precise departure from L. T. E. amongst lower quantum states has been calculated by McWhirter and Hearn (1963) by solving the appropriate set of rate equations which describe the population and depopulation of each bound state. These authors express their results in terms of two coefficients $r_o(n)$ and $r_1(n)$. The term containing $r_1(n)$ is negligible here, and we have $\frac{N_n}{\omega_n} = r_o(n) \frac{N_n}{\omega_n}^{LTE}$. Taking values of $r_o(n)$ from the tables of McWhirter and Hearn (1963) and values of $\frac{N_n}{\omega_n}^{LTE}$ from an extrapolation of the straight line of best fit to the higher bound states (fig. 2), we have calculated the theoretical values of $\frac{N_n}{\omega_n}$ shown in fig. 2, joined together by a series of straight lines for ease of identification. Errors in these values, which are greatest for the lowest states, are due to errors in the measured values of T_e and N_e. There is fair agreement between the theoretical and experimental values of $\frac{N_n}{\omega_n}$ except for the lowest excited states where absorption of Lyman radiation would be expected to elevate the densities above those predicted by the theory of McWhirter and Hearn (1963), which is for an optically thin plasma. Note that at x = 2.8 mm the temperature has fallen below the lowest value considered by McWhirter and Hearn (1963) and no theoretical points can be included for this distance. The population inversion which is observed amongst states $n \approx 2 - 5$ at x = 2.8 mm is not unexpected at the relatively low temperatures encountered this far from the target. A calculation indicates that the gain for a transition such as CVI (2-3) 182 Å, as a result of this inversion, is only $\sim 10^{-5}$ cm^{-1} (Irons and Peacock, 1974).

Finally, it might be noted that the (Debye) reduction in the ionisation potential, of ~ 1 eV (see eg Griem, 1964) has a negligible effect on any of the present results.

4.3 Plasma Parameters

Temperature and density measurements, representing time-averaged values, are shown in Table 1. The electron temperature has been measured as described in section 4.2 and illustrated in fig. 2, i.e. from the slope of the free-bound continuum (at x = 1.0 mm) and from the Saha-Boltzmann equation fitted to the higher bound states (at x = 1.6 and 2.8 mm). The continuum measurement is more accurate because of the greater range of energy (relative to the mean thermal energy) covered by the available experimental points.

Electron and ion densities have been deduced from the values of $\frac{N_n}{\omega_n}$ shown in fig. 2, viz. the Saha-Boltzmann equation fitted to the higher bound states and extrapolated to the ordinate, gives a value of $\frac{N_\infty}{\omega_\infty}$ which according to eqn 5 is related to T_e (which is known) and to the product $N_e N(C^{6+})$ by

$$\frac{N_\infty}{\omega_\infty} = \frac{N_e}{2} \frac{N(C^{6+})}{\omega_\iota} \left(\frac{h^2}{2\pi mkT_e} \right)^{\frac{3}{2}} . \qquad (7)$$

The product $N_e N(C^{6+})$ deduced by means of eqn (7) has been interpreted, in conjunction with the product $N_e N(C^{5+})$ deduced from the absolute intensity of CV(6-7) 4945 Å and with the equation of charge neutrality, to give the individual densities shown in Table 1. Note that the present CV results are somewhat less comprehensive than those for CVI, and that for the deduction of $N_e N(C^{5+})$ from CV(6-7) 4945 Å we have assumed a value of T_e equal to that deduced from the CVI radiation. This assumption is consistent with the results of Boland

et al (1968) and Irons (1973) for a similar plasma and is also consistent with the one measurement of T_e for CV which was made in the present case, from the CV free-bound continuum at x = 1.0 mm, of ~ 27 eV (compared to ~ 38 eV for CVI).

The above deduction of densities from line intensities largely follows the procedure reported for a similar plasma by Irons (1973) in which paper it was pointed out that densities deduced in this way are in factor-of-two agreement with those deduced from Stark broadening and from interferometry. The error limits indicated in Table 1 represent errors in measurement and in the interpretation procedure.

Table 1

Plasma Parameters

Distance (x) from target (mm)	T_e (eV)	N_e (10^{18} cm^{-3})	$N(C^{6+})$ (10^{17} cm^{-3})	$N(C^{5+})$ (10^{17} cm^{-3})
1.0	38^{+4}_{-4}	$4^{+1.5}_{-1.5}$	$2^{+0.7}_{-0.7}$	6^{+2}_{-2}
1.6	17^{+8}_{-5}	$0.9^{+.5}_{-.3}$	$0.5^{+.3}_{-.15}$	$1.2^{+.7}_{-.4}$
2.8	9^{+5}_{-2}	$0.17^{+.11}_{-.05}$	$0.08^{+.06}_{-.03}$	$0.17^{+.11}_{-.04}$

For the analysis to follow it is adequate to use the parameter values in Table 1 which represent averages in time and in space normal to the x axis (for a discussion of the variation in time and space in a similar plasma, see Irons, 1973).

4.4 Recombination

The progressive departure from L. T. E. amongst lower excited states (fig. 2) is indicative of the fact that there is a nett downwards flow of electrons through the excited states to the ground state, ie is indicative of the fact that the plasma is in a state of recombination.

The rate of electronic recombination of C^{6+} to C^{5+}, denoted by $\dot{N}(C^{6+})$ (not to be confused with the nett rate of decay of $N(C^{6+})$ which will be shown to be due mainly to the volume expansion), has been deduced from eqn 1 by substituting values of N_e, $N(C^{6+})$ and $N(C^{5+})$ from Table 1 and values of N_n, n = 2-8, from fig. 2 (quantum states n > 8 can be shown to contribute a negligible amount to $\dot{N}(C^{6+})$). Table 2 shows values of $\dot{N}(C^{6+})$ deduced at x = 1.0, 1.6 and 2.8 mm from the target with $n' = 4$, 4 and 3 respectively.

Table 2

Recombination Rates

Distance (x) from target (mm)	$\dot{N}(C^{6+})$ $(cm^{-3}s^{-1})$
1.0	$3.0 \pm 1 \times 10^{24}$
1.6	$1.2 \pm .4 \times 10^{24}$
2.8	$1.7 \pm .8 \times 10^{23}$

The errors listed in Table 2 have their origin in the experiment and do not include errors in the formulation of the collisional rate coefficients which appear in eqn 1 and which may be substantial (see the discussions in Bates et al, 1962a; Stabler, 1964; and Drawin, 1969). On the other hand errors in the radiative rate coefficients are negligible (for hydrogen-like ions). With the above choice of n', an additional error is therefore to be expected in $\dot{N}(C^{6+})$ at x = 1.0 mm where the collisional terms dominate the radiative terms in eqn 1; this error is smaller at x = 1.6 mm where the collisional and radiative terms are comparable and is negligible at x = 2.8 mm where the radiative terms dominate. Again, with the above choice of n', the negative terms on the right hand side of eqn 1 (which represent excitation plus negligible direct ionisation from states below n) amount to $\sim 40\%$ of the positive terms (which represent de-excitation plus direct recombination to states below n) at x = 1.0 mm, and to $\sim 10\%$ at x = 1.6 mm and $< 1\%$ at 2.8 mm. It follows that only at x = 1.0 mm are the recombination rates seriously affected by the values of density for the lower bound states and hence by the correction for opacity (section 4.1.1).

At x = 1.0 mm, the free-bound continuum can be detected, and the rate of two-body (radiative) recombination to the ground state can be deduced from the absolute continuum intensity. As with the analysis in section 4.1, absolute intensities are assigned essentially by the method of branching ratios, from the line pairs CVI(1-7), (6-7) and CVI(1-8), (7-8)). We have

$$\left.\begin{array}{l}\text{Rate of two-body recombination} \\ \text{to the ground state}\end{array}\right\} = 4\pi \int_{\nu_1}^{\infty} \frac{\varepsilon(\nu)}{h\nu}\, d\nu \qquad (8)$$

$$= 0.70 \pm 0.25 \times 10^{24}\ \text{cm}^{-3}\,\text{s}^{-1} \quad \text{at x = 1.0 mm}$$

where $\varepsilon(\nu)$ denotes the absolute intensity (ergs $s^{-1} cm^{-2} s^{-1}$ per unit frequency interval) of the measured free-bound continuum, and ν_1 denotes the frequency of the Lyman continuum edge. It is interesting to note that, at x = 1.0 mm, two-body capture to the ground state amounts to $\sim 25\%$ of the nett recombination rate (compare equation 8 with Table 2). With increasing distance from the target the intensity of the

free-bound continuum decreases relative to the line spectrum, reflecting the decreasing importance of two-body compared to three-body recombination.

Finally, a simple calculation based on the recombination rates in Table 2 and the known plasma streaming velocity (2.5×10^{7} cm s^{-1}, see section 3) shows that the density decay between x = 1.0 and 2.8 mm through recombination alone would be $\sim 6 \times 10^{15}$ cm^{-3}. Since this is much smaller than the observed decay of $\sim 3.8 \times 10^{18}$ cm^{-3} we conclude that volume expansion and not recombination is mainly responsible for the density decay between x = 1.0 and 2.8 mm.

4.4.1 Recombination Rate Coefficient

The recombination coefficient α ($cm^{-3} s^{-1}$) for the electronic recombination of C^{6+} to C^{5+} is defined by the equation

$$\dot{N}(C^{6+}) = - \alpha N_e N(C^{6+}) \quad . \tag{9}$$

More precisely, a term $+ S N_e N(C^{5+})$ representing collisional ionisation from C^{5+} to C^{6+} should be included on the right hand side of eqn 9, but this can be shown to be negligible at the rather low temperatures of interest here. It is customary to regard the absorption of Lyman line radiation (ie. photo-excitation) as a reduction to the term $\alpha N_e N(C^{6+})$ rather than as an addition to the term $S N_e N(C^{5+})$. Values of α have been calculated from eqn 9 (see column A of Table 3), using values of $\dot{N}(C^{6+})$ from Table 2 and values of $N_e N(C^{6+})$ deduced from spectral line intensities (eqn 7). It might be noted that, since both $\dot{N}(C^{6+})$ and $N_e N(C^{6+})$ are deduced from spectral intensities, the ratio of the two, namely α, is independent of absolute intensities and of the value used for the plasma depth and is dependent only on the relative intensity calibration. The error limits to the experimental values of α (see Table 3) increase with increasing distance from the target because of the greater difficulty in measuring the smaller spectral intensities at large x. The values of α at x = 1.6 mm and particularly x = 2.8 mm are, however, inherently the more accurate because of the dominance of radiative over collisional terms (see the discussion of errors following Table 2).

Table 3

Recombination coefficient α (10^{-11} cm^3 s^{-1}), for the electronic recombination of C^{6+} to the hydrogen-like C^{5+}.

Distance (x) from target (mm)	Experiment	Theory					
		Optically thin				Optically thick	
	A	B	C	D	E	F	G
1.0	$.33^{+.08}_{-.08}$	$.72^{+.1}_{-.1}$	$.55^{+.1}_{-.1}$	$.66^{+.1}_{-.1}$	$.22^{+.02}_{-.02}$	$.20^{+.05}_{-.05}$	$.21^{+.05}_{-.05}$
1.6	$2.5^{+.5}_{-.5}$	$2.1^{+1}_{-.5}$	$1.8^{+.9}_{-.7}$	$1.8^{+.9}_{-.7}$	$.40^{+.08}_{-.10}$	$1.5^{+1}_{-.8}$	$1.6^{+1}_{-.8}$
2.8	13^{+4}_{-4}	6^{+3}_{-2}	4.2^{+2}_{-2}	$3.0^{+1.2}_{-.9}$	$.60^{+.12}_{-.17}$	$3.9^{+1.1}_{-1.8}$	$3.0^{+1.2}_{-.9}$

A this paper

B Bates et al (1962a) optically thin

C, F Drawin (1969) optically thin (C), and optically thick to all Lyman lines (F)

D, G Mewe (1970) optically thin (D), and optically thick to L_α (G)

E Two-body recombination to all bound states (the limit $\eta(c) = 0$ of Bates et al, 1962a)

In a similar way the rate of purely radiative recombination to the ground state, namely $\beta(1)\, N_e\, N(C^{6+})$, can be equated to the measured rate (eqn 8), to give a value for $\beta(1)$, which again is dependent only on the relative intensity calibration. If we again use the value of $N_e\, N(C^{6+})$ deduced from spectral line intensities we find

$$\beta(1) = .98 \pm .2 \times 10^{-12} \text{ cm}^3 \text{ s}^{-1} \qquad \text{at } x = 1.0 \text{ mm} .$$

This value of $\beta(1)$ is in good agreement with the theoretical value $.83 \pm .05 \times 10^{-13} \text{ cm}^3 \text{ s}^{-1}$ of Seaton (1958) for $T_e = 38$ eV.

Also shown in Table 3 are theoretical values of α, calculated from the collisional-radiative theories of Bates et al (1962), Drawin (1969) and Mewe (1970), using the values of N_e and T_e in Table 1. The error limits to the theoretical values of α increase with increasing x because of the greater uncertainty in the plasma parameters at large x, and also because of the stronger dependence of α on the plasma parameters, approaching $N_e\, T_e^{-9/2}$ (see below).

As regards the theoretical values of α in Table 3 (columns B - G) we see that:-

(i) columns B, C and D give collisional-radiative values of α for the case of an optically thin plasma, and at each distance the three values of α are in fair agreement with one another (the non-equality of these values can be attributed to the different expressions for the collisional rate coefficients used by the different authors, and in the case of Mewe to his simplified energy level scheme).

(ii) Mewe (1970) gives collisional-radiative values of α for varying degrees of opacity to L_α, described by a factor T_{21} which takes values from 1 (optically thin to L_α) to 0 (optically thick to L_α). Because of the anisotropic nature of the streaming plasma it is difficult for us to assign a value to T_{21}. Consequently we consider the two extreme cases

$T_{21} = 1$ (column D) and $T_{21} = 0$ (column G). At x = 1.6 and 2.8 mm the values of α in columns D and G are approximately equal. This is because the minimum rate of de-excitation which determines the nett recombination rate (see Byron et al, 1962) occurs at n = 4 and is not influenced by any changes in the bound state density N_2 brought about by the absorption of L_α. At x = 1.0 mm however this minimum occurs at n = 3 and is affected by the absorption of L_α; so we find that α for $T_{21} = 0$ is only one-third the value of α for $T_{21} = 1$. Note that the absorption of other Lyman lines in addition to L_α has a negligible effect on α (this may be seen by comparing column G with column F, which is for the case (from Drawin, 1969) of a plasma optically thick to all Lyman lines).

(iii) Column E, which is included here purely for comparison purposes, shows the rate coefficient for two-body recombination onto all bound states in the absence of any collisional processes ie. it is the limit $\eta(c) = 0$ of Bates et al 1962a (the corresponding rate coefficients from Drawin, 1969 and Mewe, 1970, differ from those of Bates et al by less than 30%). The nett recombination cannot be analysed simply as the sum of a two-body term plus a three-body term because of the interactive role of the various collisional and radiative processes. Some indication, however, of the contribution from two-body capture processes to the nett recombination may be obtained from a comparison of column E with the other theory columns in Table 3, viz. two-body processes acting alone would cause the recombination of C^{6+} to proceed at a rate $\gtrsim$ 30% of the collisional radiative value at x = 1.0 mm (the exact percentage depends on the opacity), decreasing to $\sim$ 20% at x = 1.6 mm, and $\sim$ 15% at x = 2.8 mm. This trend for two-body recombination to become

progressively less important compared to three-body recombination with increasing distance from the target can be explained in terms of the N_e and T_e dependence of the respective rate coefficients (see below). Finally, we might note again that the measured rate of two-body recombination to the ground state at x = 1.0 mm (eqn 8) amounts to $\sim$ 25% of the nett recombination rate (Table 2).

Comparison of the experimental and theoretical values of α in Table 3 shows that:-

(a) at x = 1.0 mm the experimental value of α is significantly smaller than the (collisional-radiative) theoretical values for an optically thin plasma, but not as small as the theoretical value for a plasma optically thick to L_α. An examination of the theoretical expressions of Mewe (1970) shows that L_α would have to be strongly absorbed indeed ($T_{21} \lesssim 0.001$) before the optically-thick-to-L_α value would be expected to be relevant, and such a value of T_{21} is considerably smaller than the factor of $\sim$ 0.1 noted (section 4.1) for the self-absorption of L_α normal to the x axis.

(b) at x = 1.6 mm all the collisional-radiative theories give approximately the same value of α, which is not dependent on the self-absorption of L_α, and which is in good agreement with the experimental value.

(c) at x = 2.8 mm where the recombination is due almost entirely to three-body capture processes (see (iii) above), and is independent of opacity conditions, the experimental value of α is two-to-four times greater than the various theoretical values, although there is some measure of agreement with the theoretical value of Bates et al (1962a) when one allows for the rather large error limits.

Finally we might note that the values of N_e, T_e reported here (Table 1) can be fitted reasonably well to the relationship $N_e T_e^{-3/2}$ = constant, which describes an adiabatically expanding ideal gas (as also observed by Boland et al, 1968, under similar conditions). The rates of two-body and three-body recombination vary as $N_e N(C^{6+}) T_e^{-3/4}$ and $N_e^2 N(C^{6+}) T_e^{-9/2}$ respectively, and these, upon substitution of $N_e T_e^{-2/3}$ = constant, become $N_e^{-1/8} N(C^{6+})$ and $N_e^{-1} N(C^{6+})$ respectively. Clearly, since density decreases rapidly with distance from the target, the rate of two-body recombination decreases much more rapidly than does the rate of three-body recombination (until at distances $\gtrsim$ 2.8 mm two-body recombination is negligible - see (iii) above). Furthermore, if we put $N_e = \hat{Z} N(C^{6+})$, we see that the rate of three-body recombination becomes proportional to $\hat{Z}$, ie. remains constant with distance, provided the recombination is not so great that $\hat{Z}$ changes and provided, of course, that the expansion remains adiabatic. Note that, once significant recombination does occur, ionisation energy will be transferred to the free electrons by the processes of three-body recombination and the expansion will then cease to be adiabatic (eg. Rumsby and Paul, 1973).

5. Conclusion

A grazing incidence spectrograph has provided a photographic record of the Lyman line and free-bound continuum spectrum of CVI in the plasma produced by the laser irradiation of polyethylene $(C_2H_4)_n$ in vacuum (fig. 1). This has led to a measurement of the relative distribution of electrons amongst bound energy states of C^{5+}, at distances of 1.0, 1.6 and 2.8 mm from the target (fig. 2) which has been put on an absolute basis essentially by the method of branching ratios, from simultaneous observations

of the lines CVI(6-7) 3434 Å and CVI(7-8) 5290 Å. Local thermal equilibrium (L. T. E.) is shown to be attained for bound states equal to and above a certain principal quantum number n which varies with the plasma parameters, from n - 4 at 1.0 mm to n - 6 at 2.8 mm. The attainment of L. T. E. is most conclusively demonstrated at 1.0 mm where a comparison can be made with the distribution of electrons amongst free energy states, as deduced from the CVI Lyman free-bound continuum. The departure from L. T. E. amongst lower excited states becomes progressively marked at the smaller temperatures further from the target, until at 2.8 mm a population inversion amongst states of principal quantum number 2 - 5 is observed.

Over the region 1.0 - 2.8 mm from the target, the decay of (free) electron density and temperature is approximately adiabatic, and ranges from $4 \times 10^{18} cm^{-3}$ to $1.7 \times 10^{17} cm^{-3}$ and from 38 eV to 9 eV respectively. Electron and ion densities, as well as the electron temperature, have all been deduced from spectral intensities (Table 1) and have been used in conjunction with bound state densities to deduce values for the recombination rate (Table 2) and for what may well be the first determination of the recombination rate coefficient of C^{5+} (Table 3).

Recombination rates in the present rather extreme and rapidly varying plasma conditions are complicated by the contribution from self absorption of (mainly) L_α at the higher densities and by the loss in exposure at the lower densities. At intermediate densities where these two factors are less important (ie. at x = 1.6 mm) the value deduced for the collisional-radiative recombination coefficient is in good agreement with theory (Table 3). A value for the coefficient of purely two-body recombination to the ground state has been deduced from the intensity of the free-bound continuum relative to the line intensities from those higher bound states in L. T. E., and is in good agreement with theory (section 4.4.1).

The functional dependence of recombination on density and temperature is such that in the plume of a laser-produced plasma, expanding adiabatically, the rate of two-body recombination has its greatest value close to the target and decreases rapidly with distance from the target, becoming negligible compared to three-body recombination at distances greater than a few millimetres in the present case.

The method employed here to determine recombination rates (described in section 1) is based on a calculation of the various atomic processes which contribute to the recombination. It is perhaps the most suitable method for a laser-produced plasma where recombination is only a minor cause of density decay and where the competing cause of density decay (the volume expansion) can only be calculated with limited precision from plasma models. The method may be applied to all hydrogen-like ions, and indeed to non hydrogen-like ions provided the necessary radiative and collisional de-excitation rate coefficients are known with adequate precision. It is not essential to use the Lyman line spectrum to measure the bound state densities. The Balmer line spectrum has the advantage that it is less affected by opacity, but it has the disadvantage that it is less intense, that probably fewer series members can be detected and that the first excited state is inaccessible to measurement.

Acknowledgements

We would like to thank Mr. A.W. Waller (A.W.R.E. Aldermaston) for supplying the redesigned entrance slit assembly for the grazing incidence spectrograph, and Mr. A.H. Jones for his assistance with the construction of the laser, for its day-to-day operation, and for his general assistance with the experiment. We are also grateful to Dr. R.W.P. McWhirter (of the Astrophysics Research Unit, S.R.C.) for his criticism of the manuscript.

References

Baravian G., Benattar R., Bretagne J., Godart J. L. and Sultan G. 1973 Zeit. fur Physik 260, 121-130.

Basov N. G., Boiko V. A., Gribkov V. A., Zakharov S. M., Krokhin O. N., and Sklizkov G. V., 1969 Ninth Int. Conf. on Phenomena in Ionised Gases, Bucharest, 333.

Bates D. R., Kingston A. E. and McWhirter R. W. P., 1962a, Proc. R. Soc. A267, 297-312.

Bates D. R., Kingston A. E. and McWhirter R. W. P., 1962b, Proc. R. Soc. A270, 155-167.

Boland B. C., Irons F. E. and McWhirter R. W. P., 1968, J. Phys. B: Atom. Molec. Phys. 1, 1180-91.

Burgess D. D., Fawcett B. C. and Peacock N. J., 1967, Proc. Phys. Soc. 92, 805-16.

Byron S., Stabler R. C. and Bortz P. I., 1962, Phys. Rev. Letts 8, 376-9.

Cooper J., 1966, Reports on Progress in Physics 29, 35-130.

Drawin H. W., 1969, Z. Physik 225, 470-82 (also EUR-CEA-FC-510 available as ASIS - NAPS - 00426 document).

Gabriel A. H., Swain J. R. and Waller W. A., 1965, J. Sci. Instrum. 42, 94-7.

Griem H. R., 1964, Plasma Spectroscopy, McGraw-Hill.

Hearn A. G., 1966, Proc. Phys. Soc. 88, 171-91.

Hinnov E., 1966, Phys. Rev. 147, 197-200.

Hobby M. and Peacock N. J., 1973, J. Phys. E : Sci. Instrum. 6, 854-7.

Irons F. E., McWhirter R. W. P. and Peacock N. J., 1972, J. Phys. B : Atom. Molec. Phys. 5, 1975-87.

Irons F. E., 1973, J. Phys. B : Atom. Molec. Phys. 6, 1562-81.

Irons F. E. and Peacock N. J., 1973, J. Phys. E : Sci. Instrum. 6, 857-62.

Irons, F. E. and Peacock, N. J. 1974 to be published.

Irons F.E., 1975, to be published.

Mattioli M., 1971, Plasma Physics 13, 19-28.

Mattiol M. and Véron D., 1969, Plasma Physics 11, 684-6.

Mattioli M. and Véron D., 1971, Phys. Fluids 14, 717-21.

McWhirter R.W.P., 1965, 'Plasma Diagnostic Techniques' Eds. R.H. Huddlestone and S. L. Leonard (N.Y. Academic Press) Chapter 5.

McWhirter R.W.P. and Hearn A.G., 1963, Proc. Phys. Soc. 82, 641-54.

Menzel D.H. and Pekeris C.L., 1935, M.N.R.A.S. 96, 77-111.

Mewe R., 1970, Z. Naturforschg. 25a, 1798-1803.

Morgan F.J., Gabriel A.H. and Barton M.J., 1968, J. Phys. E : Sci. Instrum. 1, 998-1002.

Peacock N.J. and Pease R.S., 1969, J. Phys. D : Appl. Phys. 2, 1705-17. (see also Irons F.E., Peacock N.J. and Pease R.S., 1972, Sov. J. of Qu. Elect. 2, 13-17).

Robben F., Kunkel W.B., and Talbot L., 1963, Phys. Rev. 132, 2363-71.

Rumsby P.T. and Paul J.W.M. 1973 Culham Preprint CLM-P340.

Seaton M., 1959, M.N.R.A.S. 119, 81-9.

Seka W., Schwob J.L. and Breton C., 1970, J.A.P. 41, 3440-1.

Speer R.J. and Turner D. 1973, Proc. of the International Symposium for Synchrotron Radiation Users, Daresbury, 106-14.

Stabler R.C., 1964, Phys. Rev. 133A, 1268-73.

Stevefelt J. and Robben F., 1972, Phys. Rev. A5, 1502-15.

Tonon G.F., 1972, IEEE Trans. Nucl. Sci. NS-19, 172-83.

Zel'dovich Ya. B. and Raizer Yu. P., 1967, Physics of Shock Waves and High Temperature Hydrodynamic Phenomena (Academic Press) 2, 571.

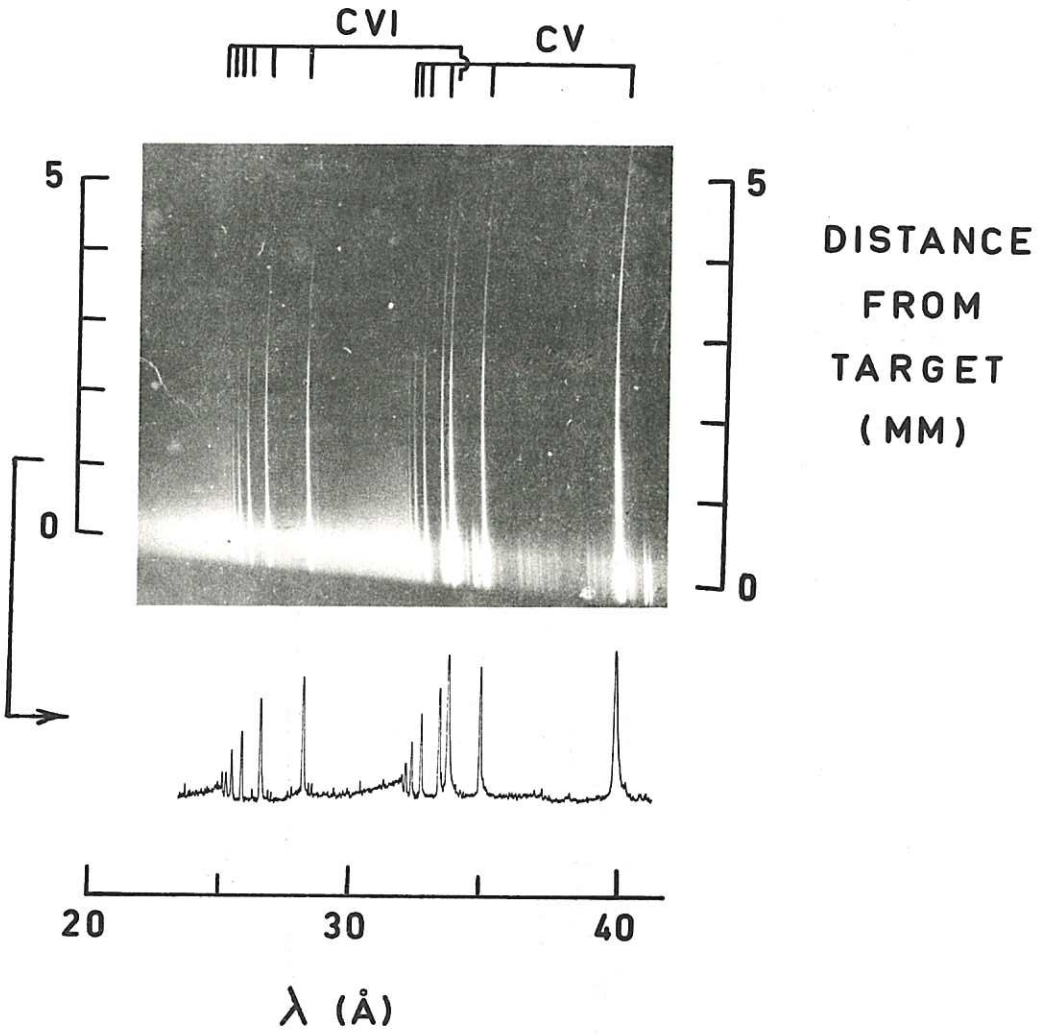

Figure 1. The Lyman spectrum of carbon VI (and V) in the plasma produced by the laser irradiation of polyethylene, as recorded with a grazing incidence spectrograph, with spatial resolution of 0.5 mm parallel to the target normal. Also shown is a spectrophotometer scan corresponding to a distance of 1.0 mm from the target, with seven members of the CVI Lyman series clearly visible.

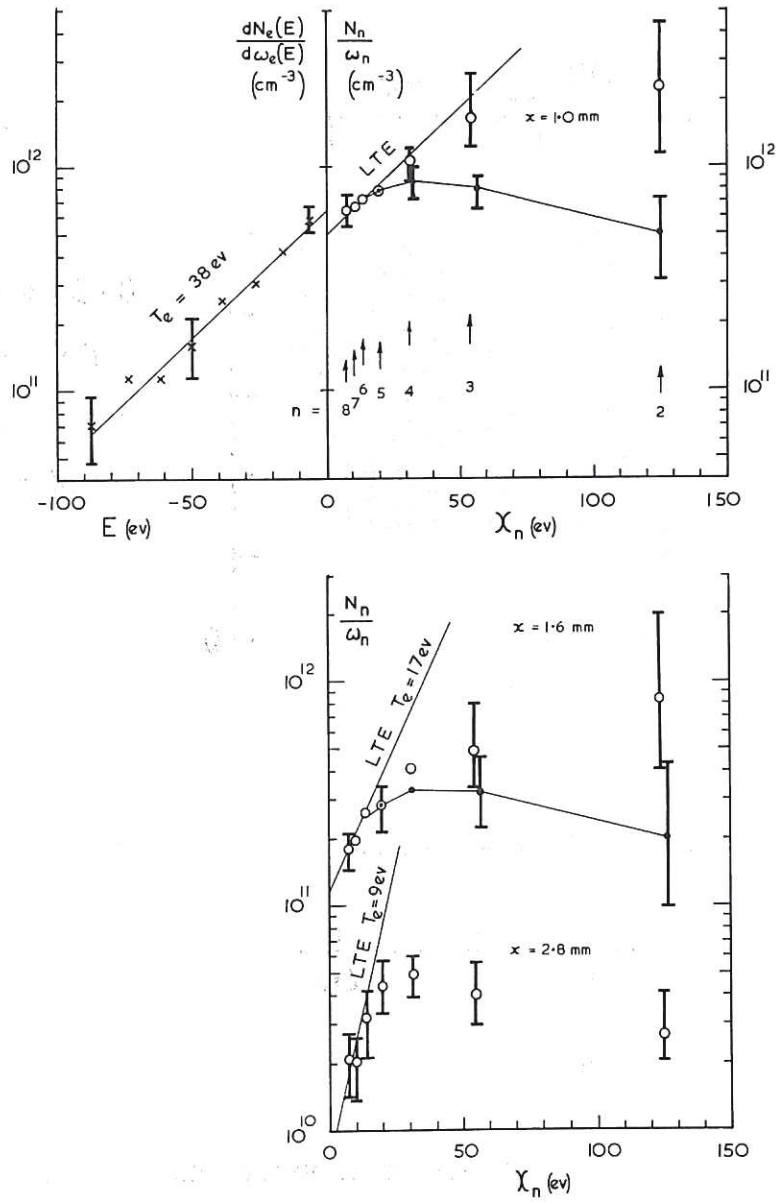

Figure 2. Three graphs, corresponding to distances of x = 1.0, 1.6 and 2.8 mm from the target, show the distribution of electrons amongst free energy states ( ) as deduced from the CVI free-bound continuum and amongst excited bound energy states of C^{5+} ( ) as deduced from the CVI Lyman line intensities corrected for self absorption. Theoretical values ( ) for an optically thin plasma (McWhirter and Hearn, 1963), calculated using values of N_e and T_e deduced from the higher excited state populations, are included and are joined by straight lines for ease of identification. In addition to the relative errors shown on the experimental points in the figure, the absolute value of each point is uncertain by a further $\pm$ 30% arising from the method of assigning absolute values.